Membrane-coated glass electrodes for stable, low-noise electrophysiology recordings in *Drosophila* central neurons

Angelica T. Jameson[1,†], Lucia K. Spera[1,†], Dieu Linh Nguyen[1], Elizabeth M. Paul[1], Masashi Tabuchi[1]

[1]Department of Neurosciences, Case Western Reserve University School of Medicine, Cleveland, OH, United States.

Abstract

Background—Electrophysiological recording with glass electrodes is one of the best techniques to measure membrane potential dynamics and ionic currents of voltage-gated channels in neurons. However, artifactual variability of the biophysical state variables that determine recording quality can be caused by insufficient affinity between the electrode and cell membrane during the recording.

New method—We introduce a phospholipid membrane coating on glass electrodes to improve intracellular electrophysiology recording quality. Membrane-coated electrodes were prepared with a tip-dip protocol for perforated-patch, sharp-electrode current-clamp, and cell-attached patch-clamp recordings from specific circadian clock neurons in *Drosophila*. We perform quantitative comparisons based on the variability of functional biophysical parameters used in various electrophysiological methods, and advanced statistical comparisons based on the degree of stationariness and signal-to-noise ratio.

Results—Results indicate a dramatic reduction in artifactual variabilities of functional parameters from enhanced stability. We also identify significant exclusions of a statistically estimated noise component in a time series of membrane voltage signals, improving signal-to-noise ratio.

Comparison with existing methods—Compared to standard glass electrodes, using membrane-coated glass electrodes achieves improved recording quality in intracellular electrophysiology.

Conclusions—Electrophysiological recordings from *Drosophila* central neurons can be technically challenging, however, membrane-coated electrodes will possibly be beneficial for reliable data acquisition and improving the technical feasibility of axonal intracellular activities

measurements and single-channel recordings. The improved electrical stability of the recordings should also contribute to increased mechanical stability, thus facilitating long-term stable measurements of neural activity. It is, therefore, possible that membrane-coated electrodes will be useful for any model system.

Keywords

DN1p; Drosophila; electrophysiology; patch-clamp recording; membrane potential

1. Introduction

Electrophysiological recording with a glass electrode is a traditional but still extremely powerful technique to measure membrane potential dynamics and ionic currents of voltage-gated channels in the neuron (Adrian, 1926; Hamill et al., 1981; Hodgkin and Huxley, 1952; Neher and Sakmann, 1976). Glass electrodes can provide the highest temporal resolution of the biophysical kinetics of neuronal activity, allowing us to quantitatively study the temporal structure of the membrane potential and the biophysical dynamics of ionic currents. There are two main types of glass electrodes used in electrophysiology: sharp microelectrodes and patch-clamp electrodes (Li et al., 2004; Staley et al., 1992). Classical intracellular recording configuration can be made by inserting sharp microelectrodes into the cell membrane (Svoboda et al., 1999; Thomas, 1977), and enhanced capabilities of sharp recording electrodes have been obtained (Angle and Schaefer, 2012; Jayant et al., 2017; Jayant et al., 2019; Robinson et al., 2012). Patch-clamp electrodes, on the other hand, can be used in various configurations (Hamill et al., 1981; Sakmann and Neher, 1984; Sigworth, 1986), including cell-attached patch-clamp recording (Hasebe and Yoshino, 2016; Nakamura and Yoshino, 2013; Neher and Sakmann, 1976; Sigworth and Neher, 1980), whole-cell patch-clamp recording (Cahalan and Neher, 1992; Li, 2008), and perforated patch-clamp recording (Fan and Palade, 1998; Hess et al., 2021; Horn and Marty, 1988; Lindau and Fernandez, 1986; Nakamura and Yoshino, 2013; Sarantopoulos et al., 2004). The formation of a tight electrical seal between the electrode and cell membrane is critical for obtaining high-quality recordings, regardless of any method type (Li, 2008; Priel et al., 2007; Suchyna et al., 2009). Leak conductance can occur if the seal is not sufficiently tight and, in turn, introduce unwanted noise and artifacts into the recorded signals, compromising the accuracy of the measurements (Lei et al., 2020). To overcome this problem, we introduce a phospholipid membrane coating on glass electrodes, inspired by the classical "tip-dip method" (Sokabe et al., 1991; Thieffry et al., 1992). The tip-dip method is one of the patch-clamp techniques used in an artificial bilayer system for *in vitro* ion channel research. This method involves dipping a pipette tip into a lipid solution and then touching it to a substrate, which creates a lipid bilayer on the tip of the patch pipette. The patch pipette is then lowered into a solution containing the channel of interest, and the channel can be studied using patch-clamp electrophysiology. The secure electrical seal achieved by this tip-dip method is based on a hydrophobic interaction; however, our method, described in the present study, is based on a hydrophilic interaction. Here, we describe a new membrane-coated electrode that shows significantly improved recording stability using a specific type of circadian clock neuron called DN1ps (Lamaze and Stanewsky, 2019; Shafer and Keene, 2021; Tabuchi, 2023; Tabuchi et al., 2021), which regulates sleep in *Drosophila* (Guo et

al., 2018; Guo et al., 2016; Lamaze et al., 2018). We demonstrate reduced variabilities of functional parameters and the technical feasibility of simultaneous measurements of multiple axonal intracellular activities and single-channel recordings with lowered noise in the *Drosophila* central brain.

2. Methods

Lipid preparation

A lipid membrane was made based on egg yolk lecithin (440154; Sigma-Aldrich) and cholesterol (C8667; Sigma-Aldrich), as previously described (Hamada et al., 2014). Egg yolk lecithin (7.6 g/L) and cholesterol (2 mM) were prepared by dissolving in a solvent of hexane (34859; Sigma-Aldrich) and acetone (270725; Sigma-Aldrich) using an ultrasonication machine for 1 hour at room temperature. Hexane and acetone were then evaporated by pressure injection of an inert nitrogen, following additional incubation under the decompression chamber. After the complete removal of the hexane/acetone solvent, egg yolk lecithin and cholesterol were transferred to a mixture of liquid paraffin/squalene (7/3, v/v), and incubated at 80°C overnight. The next day, the prepared lipid was immediately used for electrode preparation.

Electrode preparation

Patch-electrodes (12 – 20 MΩ) were fashioned from thoroughly cleaned borosilicate glass capillaries (OD/ID: 1.2/0.68mm) with a Flaming-Brown puller (p-97; Sutter Instrument, CA, USA). The 12 – 20 MΩ tuning was chosen to make the shank narrower and the tip diameter smaller for effective data acquisition from *Drosophila* DN1 neurons, which is achieved by reducing the physical contact site of the perforating reagent on the neuronal membrane and reducing the internal circulation velocity of the perforating reagent, while being aware of potential technical issues such as series resistance compensation.

The electrode tip was polished with a microforge (MF200; World Precision Instruments, FL, USA). Sharp-electrodes (120 – 190 MΩ) were fashioned from thoroughly cleaned quartz glass capillaries (OD/ID: 1.2/0.6mm) with a laser-based micropipette puller (P-2000, Sutter instrument). To make membrane-coated electrodes, we first dipped the electrode tip into an internal electrode solution in a custom-made reservoir. The level at which the glass electrodes were immersed in the internal electrode solution was carefully limited to the minimum depth using a micromanipulator (U-12C; Narishige, Japan) or a travel translation stage (MS1S; Thorlabs, USA). We then loaded the prepared lipid solution onto the surface of the internal electrode solution. Phospholipids are amphipathic molecules, meaning they have both hydrophilic and hydrophobic regions. Thus, a single phospholipid monolayer is expected to form at the interface between the water and oil phases (Noireaux and Libchaber, 2004). After loading the minimum amount (<20 μL) of the prepared lipid solution onto the surface of the internal electrode solution, we vertically pulled up the electrode using the micromanipulator. The membrane-coated electrodes were immediately used for electrophysiological recording, following the standard backfilling of the internal electrode solution by using a microfiller (MF34G MicroFil; World Precision Instruments). The internal pipette solution with 102 mM potassium gluconate, 0.085 mM $CaCl_2$, 0.94

mM EGTA, 8.5 mM HEPES, 4 mM Mg-ATP, 0.5 mM Na-GTP, 17 mM NaCl, pH7.2 with osmolarity adjusted to 226–230 mOsm without detectable change regardless of membrane coating was used for all patch-clamp recording experiments. The internal pipette solution with 1 M KCl was used for sharp electrode intracellular recordings. These internal pipette solutions were filtered by using a syringe filter with a pore size of 0.02 μm (Anotop 10, Whatman).

Electrophysiological recordings

Drosophila preparations—All Drosophila strains were obtained from the Bloomington Drosophila Stock Center (Bloomington, IN, USA). To target and visualize DN1p neurons, R18H11-Gal4 line (BDSC: 48832) and UAS-CD4-tdGFP line (BDSC: 35836) were recombined by using standard genetic recombination techniques and used for electrophysiological recordings. Flies were fed standard Drosophila food containing molasses, cornmeal, and yeast. They were housed in a 25°C incubator (DR-36VL, Percival Scientific, Perry, IA, United States) under 12h:12h light:dark cycles and 65% humidity. Female flies were used for all experiments. All experiments were performed at 25 °C and in compliance with all relevant ethical regulations for animal testing and research at Case Western Reserve University. We performed dual electrophysiological recordings from a DN1p neuron using an *in vivo* configuration (Murthy and Turner, 2013a). The dual recording was essentially based on our previous study (Ho et al., 2022), but differed in that two electrodes were targeted to one cell (patch electrodes) or one cell type (sharp recording electrodes). All experiments were performed at ZT18–20. Flies (2–3 days old) were chilled on ice (up to 10 min) for anesthesia and placed in a dissecting chamber. Flies were dissected in a *Drosophila* physiological saline solution (101 mM NaCl, 3 mM KCl, 1 mM $CaCl_2$, 4 mM $MgCl_2$, 1.25mM NaH_2PO_4, 20.7 mM $NaHCO_3$, and 5 mM glucose; with osmolarity adjusted to 235–245 mOsm and pH 7.2), which was pre-bubbled with 95% O_2 and 5% CO_2. The glial sheath surrounding the DN1p neurons was focally and carefully removed by using sharp forceps after treatment with an enzymatic cocktail, collagenase (0.1 mg/mL), protease XIV (0.2 mg/mL), and dispase (0.3 mg/mL), at 22°C for 1 min (Nguyen et al., 2022). Using a small stream of saline, which was pressure-ejected from a large-diameter pipette, the surface of the cell body was cleaned under a dissection microscope. DN1p neurons were visualized via tdGFP fluorescence by using a PE300 CoolLED illumination system (CoolLED Ltd., Andover, UK) on a fixed-stage upright microscope (BX51WI; Olympus, Japan).

Patch-clamp recordings—Perforated patch-clamp of DN1p neurons were performed from somatic recording, as performed previously (Nguyen et al., 2022; Tabuchi et al., 2018). Escin (Fan and Palade, 1998; Hess et al., 2021; Nakamura and Yoshino, 2013; Sarantopoulos et al., 2004) was prepared as a 50 mM stock solution in water (stored up to 2 weeks at −20°C) and was added fresh into the internal pipette solution to a final concentration of 50 μM. Filling syringes were wrapped with aluminum foil, owing to the light-sensitivity of escin. Escin pipette solutions remained stable for several hours after mixing in the filling syringe, with no evidence of precipitate formation. Junction potentials were nullified prior to high-resistance seal formation. After the high-resistance seal formation, perforated patches were allowed to develop spontaneously over time.

After breakthrough became evident, as determined by the gradual development of a large capacitance transient in the seal test window, access resistance monitoring was initiated employing the membrane test function. After that point, access resistance (Ra) was monitored continuously during the final completion of perforation process, until it became stable (Ra stably < 40 MΩ). Cell-attached recordings of DN1p neurons were performed from somatic recording, based on the standard cell-attached recording configuration (Hasebe and Yoshino, 2016; Inoue et al., 2014; Shahidullah et al., 2009). For perforated clamp recordings, dual electrophysiological signals were acquired with two independent Axopatch 1D amplifiers (Molecular Devices) and sampled with Digidata 1550B (Molecular Devices) controlled by pCLAMP 11 (Molecular Devices), except for data acquisition of membrane tests made by a single electrode. For cell-attached recordings, measurement was made by a single electrode, and processed by an Axopatch 1D amplifier, sampled with Digidata 1550B (Molecular Devices) controlled by pCLAMP 11 (Molecular Devices). We used a single-step pulse change from −70 mV holding potential to +60 mV holding potential to observe single-channel membrane current (Shahidullah et al., 2009). The electrophysiological signals were sampled at 20 kHz and low-pass filtered at 1 kHz.

Sharp electrode intracellular recordings—We inserted the electrode into the region having dense tdGFP signals of the axonal regions of DN1ps in R18H11-Gal4>UAS-CD4-tdGFP flies. During the insertion process of the electrode, tdGFP signals were used for initial visual inspection, and the depth direction of insertion was determined by change of sound (Model 3300 Audio Monitor, A-M Systems) and generation of membrane potential. This process was facilitated by adding "buzz" pulses at the moment just before the electrode was about to cross the membrane. The duration of pulse was determined by "advance air shooting". If the tip of the electrode is seen through the microscope lens as physically shaking, the duration was determined to be too long. We utilized the longest duration in the range that the electrodes do not move, which was typically between 2–5 ms. Recordings of membrane potentials commenced after membrane potential was stable, as it usually takes at least several minutes to stabilize the cell membrane potential. Recordings were acquired with an Axoclamp 2B with HS-2A x 1 LU headstage (Molecular Devices), and sampled with Digidata 1550B interface, which were controlled on a computer using pCLAMP 11 software. The signals were sampled at 10 kHz and low-pass filtered at 1 kHz.

Statistical analysis of electrophysiology data

Statistical analyses were done using Prism software version 10.1.0. (GraphPad), Clampfit version 10.7 (Molecular Devices) or MATLAB 2023b (MathWorks). To compare two groups of non-simultaneously measured electrophysiological data, normally distributed data were compared using t-tests, and non-normally distributed data were compared using Mann-Whitney U-tests. For comparisons of simultaneously measured electrophysiological signals with normal distributions, paired t-tests were used. To compare more than two multiple-group comparisons, two-way ANOVA with Šídák's multiple comparisons test was used. A p-value < 0.05 is considered a statistically significant test result. Asterisks indicate p-values, where *p < 0.05, **p < 0.01, ***p < 0.001, and ****p < 0.0001. Error bars are means ± SEM averaged across experiments. Numerical values of time-series data of access resistance (Ra), membrane capacitance (Cm), membrane resistance (Rm), and membrane time constant

(Tau) were obtained from the Membrane Test tool in pCLAMP 11 (Molecular Devices). The membrane potential (Vm) variability was quantified from the standard deviation of the all-point voltage signal during the current-clamp mode. The decay time variability was quantified from the standard deviation of the time it took the voltage across the membrane to decrease to approximately 36.8% of its initial value. The input resistance variability was quantified from the standard deviation of the Vm divided by the injection current. The Augmented Dickey-Fuller (ADF) test was used to determine whether a unit root is present in a time series dataset (Chatfield, 2003; Dickey and Fuller, 1979). A unit root is a mathematical property of a time series indicating that it has a stochastic trend (Dickey, 1993; Dickey and Fuller, 1981; Granger, 1981). A Gaussian noise process is considered stationary because its statistical properties, such as mean and variance, do not change over time (Box, 1989; Chatfield, 1977). Therefore, we believe that a higher p-value in the ADF test is linked to insufficient evidence to conclude stationarity, possibly attributed to decreased Gaussian noise. The signal-to-noise ratio (SNR) of the single-channel recordings was quantified in dBc (decibels relative to the carrier wave) of a real-valued sinusoidal membrane current determined from a modified periodogram using a Kaiser window with $\beta = 38$ of the same length as the input (Proakis and Manolakis, 2006). Sample sizes were predetermined based on previous studies and technical feasibility, and one DN1 neuron was recorded per fly.

Electron microscope imaging

We used scanning electron microscope (SEM) imaging to visualize the electrode tips. Electrodes were imaged using bright field mode at 5,000x and 12,000x (2 kV, 13 pA) with a ThermoFisher Apreo 2S SEM with an Everhart–Thornley detector (Case Western Reserve University School of Engineering Swagelok Center for Surface Analysis of Materials, NSF MRI Award: 2018167).

3. Experiment

We introduce a phospholipid membrane coating on glass electrodes. Membrane-coated electrodes were prepared using a newly developed tip-dip protocol (Figure 1A). The surfaces of an uncoated glass electrode (Figure 1B) and a membrane-coated glass electrode (Figure 1C) were visualized by electron microscopy. We simultaneously compared the membrane-coated electrodes to standard glass electrodes used in patch-clamp to contest the variability of the fundamental biophysical natures in the voltage clamp mode ("membrane test") of the perforated patch-clamp recordings (Figure 2A). We excluded using the whole-cell patch-clamp recording technique because of technical difficulty in making it stable in DN1 neurons and the potentially undesirable mixing of the artificial membrane with the intracellular plasma of the cell, although we did not extensively validate this possibility. We found that the membrane-coated glass electrodes showed significantly reduced access resistance, in comparison with standard glass electrodes (Figure 2B). In addition to a reduction of access resistance, we also found a significant reduction of variability of the access resistance (Figure 2C). Correlating with this reduction of the variability of the access resistance, reduced variability was also evident in parameters of membrane capacitance (Figure 2D), membrane resistance (Figure 2E), and time constant (Figure 2F). Next, we simultaneously compared the stability of actual membrane voltage in the current

clamp mode of the perforated patch-clamp recordings (Figure 3A). Dynamic properties of membrane voltage (Vm) were quantified in current-clamp mode with hyperpolarized and depolarized stepping current injection, and membrane-coated electrodes showed reduced Vm variability, regardless of any stepping current injection (Figure 3B). Baseline "resting" Vm showed a similar reduction in its variability (Figure 3C). We reasoned that reduced Vm variability was caused by reduced noise components. Therefore, we performed the Augmented Dickey-Fuller (ADF) test, as the ADF test implies the likelihood of noise-attribution stationary components (Dickey and Fuller, 1979). The ADF test of Vm data obtained from membrane-coated glass electrodes showed a significantly higher p-value than standard glass electrodes (Figure 3D), indicating decreased Gaussian noise. We also compared action potential waveforms (Figure 3E) and phase plots (Figure 3F), plotting the first time derivative of membrane voltage dVm/dt versus Vm, and both the raw action potential Vm trace and the phase plot showed nearly overlapping patterns between uncoated and coated electrodes. We next compared the stability of membrane voltage in the current clamp mode of the sharp electrode intracellular recordings (Figure 4A). Similar to the perforated patch-clamp recordings, membrane-coated electrodes demonstrated their ability to reduce the variability of biophysical parameters, including decay time constant in response to depolarized stepping current injection (Figure 4B), input resistance (Figure 4C), and Vm following hyperpolarized prepulse stimulus (Figure 4D). Similar to the result of the perforated patch-clamp recordings, baseline "resting" Vm showed a similar reduction in its variability (Figure 4E). We then performed the ADF test to determine the influence of noise-attributed stationary components (Chatfield, 2003), and the ADF test of Vm data obtained from membrane-coated glass electrodes showed a significantly higher p-value than standard glass electrodes (Figure 4F). We also compared action potential waveforms (Figure 4G) and phase plots (Figure 4H), and similar to the results in perforated patch clamp recording, both the raw action potential Vm trace and the phase plot showed nearly overlapping patterns between uncoated and coated electrodes. Finally, we evaluated the performance of membrane-coated glass electrodes in single-channel recording. The single-channel recording was conducted by a standard cell-attached configuration (Figure 5A). Significant baseline drift occurred with the standard glass electrode during single-channel recording (Figure 5B). In contrast, reduced baseline drift was observed in the single-channel recording dataset obtained by membrane-coated glass electrodes (Figure 5C). The all-points histograms of the membrane currents also showed remarkable differences between the standard glass electrode and the membrane-coated glass electrodes. The all-points histogram of the membrane currents obtained with the standard glass electrode showed less clear identification between the close and open states (Figure 5D). On the other hand, the all-points histogram of the membrane currents obtained with the membrane-coated glass electrode showed visually distinguishable closed and open states (Figure 5E). We hypothesized that the difference was due to an increased signal-to-noise ratio (SNR) in the membrane-coated electrodes. Remarkably, we observed a significantly higher SNR in membrane-coated electrodes compared to standard electrodes (Figure 5F). We also quantified the SNR between the start and end points of the single-channel recordings and found a significant deterioration in the control electrodes, while no significant difference was found in the membrane electrodes (Figure 5G). Together, these data suggest that significantly improved recording quality

of intracellular electrophysiology from *Drosophila* brain can be achieved by using newly developed membrane-coated glass electrodes.

4. Discussion

Drosophila melanogaster is a powerful model organism for understanding the genetic mechanisms underlying neurodevelopment, neurophysiology, and neuroethology. However, in the application of intracellular electrophysiology to the adult central nervous system in vivo, *Drosophila* lagged far behind other model organisms until the pioneering development of whole-cell patch-clamp recording from antennal lobe neurons *in vivo* (Wilson et al., 2004). Intracellular electrophysiology in the adult *Drosophila* central nervous system still faces technical problems regarding the quality of recordings, which derive from unavoidable biological, artifactual, and/or technical factors (Cao and Nitabach, 2008; Flourakis and Allada, 2015; Fogle et al., 2011; Gouwens and Wilson, 2009; McCarthy et al., 2011; Murthy and Turner, 2013b; Sheeba et al., 2008). There have been substantial attempts to solve these problems, including modified protocols depending on the target cell type or specific issues being addressed (Barber and Sehgal, 2021; Fernandez-Chiappe and Muraro, 2022a, b, c, d; Flourakis and Allada, 2015; Murthy and Turner, 2013b; Roemmich et al., 2018; Ryglewski and Duch, 2012). In the present study, we demonstrate improved recording quality in intracellular electrophysiology using membrane-coated glass electrodes. The technical challenges associated with electrophysiological recordings from *Drosophila* central neurons were evident, but our study exhibits the potential benefits of using this method for data acquisition in such technically challenging model systems. To demonstrate reliable comparisons, we performed simultaneous recordings from a DN1 neuron with membrane-coated and control electrodes in most experiments. We acknowledge that this unusual recording configuration (i.e., dual recordings from a single neuron) may negatively affect membrane health. However, we believe that minimizing the physical contact between the electrode and the neuronal surface by reducing the diameter of the electrode tip may help minimize mechanical invasiveness and thus reduce membrane health concerns. While we also acknowledge that it would be difficult to thoroughly rule out the possibility of uncharacterized biophysical influences caused by this recording configurations, we believe that performing dual recordings from a single DN1 neuron is critical for comparing membrane-coated and control electrodes in terms of comparing the Vm trace of the action potential and its phase plot, both of which show nearly overlapping patterns between uncoated and coated electrodes. These results suggest that these biophysical kinetics are not affected by changing the surface material of the recording electrode. Furthermore, we demonstrate the technical feasibility of simultaneously measuring multiple intracellular activities and performing single-channel recordings with improved SNR in the *Drosophila* central brain. Furthermore, comparisons of the SNR between the start and end points of the single-channel recordings suggest that the improved SNR observed with the membrane-coated electrodes is stable over time, at least for our recording duration. Further validation of how long this coating is stable over time will be useful for quantifying the temporal stability of the coating. Our protocol for making membrane-coated electrodes was inspired by the traditional "tip-dip method" used in artificial membrane systems to study ion channels *in vitro*. Membrane potential and currents have long been recorded using intracellular

electrophysiology based on glass electrodes. Although this technique is clearly thriving in standard model systems, we believe that there are still substantial portions to optimize to be able to reliably record from technically challenging model systems, including *Drosophila* central neurons, which were used in the present study. We believe that our membrane-coated glass electrodes can help overcome this problem by improving the electrochemical affinity between the glass electrode and the neuronal membrane surface. The hydrophobic nature of glass repels hydrophilic membrane components that have been shown to be necessary for both monolayer and bilayer formation and critical membrane functions. Thus, coating hydrophobic glass surfaces with a phospholipid membrane adds hydrophilic properties, which we believe contributes to a significant reduction in the variability of biophysical parameters by eliminating artifactual noise components.

5. Limitations of the study

There may be several potential limitations to this study. First, we tested the performance of our membrane-coated electrodes only focusing on the variability of passive membrane properties based on standard electrophysiological experiments. Although the surface of a membrane-coated glass electrode was visualized by electron microscopy, the details of microstructural physical interaction between glass electrodes, membrane coating, and neuronal membrane surface remain to be elucidated. Second, we investigated the effects of our membrane-coated electrodes only on specific neuronal types of circadian clock neurons (i.e., DN1p) in *Drosophila*; whether our membrane-coated electrodes could bring functional benefit for intracellular electrophysiology of other types of neurons in *Drosophila* was not addressed in this study. Third, there is still no evidence that our membrane-coated glass electrodes can also bring benefits to other model systems. While these considerations do not affect the results shown in the present study, addressing these issues may provide more valuable insights into whether our membrane-coated glass electrodes could universally contribute to improving the quality of recordings, or are only beneficial when neurons have relatively higher leakage conductance, such as DN1p neurons (Flourakis et al., 2015; Seluzicki et al., 2014). Because this advancement not only minimizes electrical leakage to suppress artifactual variability of biophysical state variables determining recording quality, but also increases mechanical stability, protecting against external noise, we believe that the applicability of this method extends beyond *Drosophila* central neurons, suggesting its potential utility in other model systems.

6. Conclusions

Drosophila melanogaster has been used as a valuable model organism for neurosciences. Despite its importance, the application of intracellular electrophysiology to the adult central nervous system in *Drosophila* has faced challenges and lagged behind other models. The present study developed membrane-coated glass electrodes for the purpose of reducing artifactual variabilities delivered by technical difficulties of *Drosophila* electrophysiology. The developed method to achieve membrane coating is based on the modification of the classical tip-dip method of artificial membrane systems. We find that membrane-coated glass electrodes reduce the variability of biophysical parameters and eliminate artifactual noise components. This innovation holds the potential for reliable recordings in challenging

model systems such as *Drosophila* central neurons and represents a step towards optimizing intracellular electrophysiology in such contexts.

Acknowledgments

Data availability statement

The raw data supporting the conclusions of this article will be made available by the authors, without undue reservation.

References

Adrian ED. The impulses produced by sensory nerve endings: Part I. J Physiol, 1926; 61: 49–72. [PubMed: 16993776]

Angle MR, Schaefer AT. Neuronal recordings with solid-conductor intracellular nanoelectrodes (SCINEs). PLoS One, 2012; 7: e43194. [PubMed: 22905231]

Barber AF, Sehgal A. Monitoring Electrical Activity in Drosophila Circadian Output Neurons. Methods Mol Biol, 2021; 2130: 221–32. [PubMed: 33284448]

Box GEP. An Unexpected Route to Time-Series - a Citation Classic Commentary on Time-Series Analysis - Forecasting and Control by Box,G.E.P., and Jenkins,G.M. Cc/Phys Chem Earth, 1989: 22-.

Cahalan M, Neher E. Patch clamp techniques: an overview. Methods Enzymol, 1992; 207: 3–14. [PubMed: 1382186]

Cao G, Nitabach MN. Circadian control of membrane excitability in Drosophila melanogaster lateral ventral clock neurons. J Neurosci, 2008; 28: 6493–501. [PubMed: 18562620]

Chatfield C The Analysis of Time Series. Chapman and Hall/CRC: New York, 2003.

Chatfield C Introduction to Statistical Time-Series - Fuller,Wa. J Roy Stat Soc a Sta, 1977; 140: 379–80.

Dickey DA. A Statistical Test for Stability - a Citation-Classic Commentary on Likelihood Ratio Statistics for Autoregressive Time-Series with a Unit-Root by Dickey,D.A., Fuller,W.A. Cc/Art Human, 1993: 16-.

Dickey DA, Fuller WA. Distribution of the Estimators for Autoregressive Time-Series with a Unit Root. J Am Stat Assoc, 1979; 74: 427–31.

Dickey DA, Fuller WA. Likelihood Ratio Statistics for Autoregressive Time-Series with a Unit-Root. Econometrica, 1981; 49: 1057–72.

Fan JS, Palade P. Perforated patch recording with beta-escin. Pflugers Arch, 1998; 436: 1021–3. [PubMed: 9799421]

Fernandez-Chiappe F, Muraro NI. Dissection of Drosophila Adult Brains for Patch-Clamping Neurons. Cold Spring Harb Protoc, 2022a; 2022: Pdb prot107935.

Fernandez-Chiappe F, Muraro NI. Patch-Clamping Drosophila Brain Neurons. Cold Spring Harb Protoc, 2022b; 2022: pdb prot107936.

Fernandez-Chiappe F, Muraro NI. Patch-Clamping Fly Brain Neurons. Cold Spring Harb Protoc, 2022c; 2022: Pdb top107796.

Fernandez-Chiappe F, Muraro NI. Preparation of Pipettes and Pipette-Filling Devices for Patch-Clamping Drosophila Neurons. Cold Spring Harb Protoc, 2022d; 2022: pdb prot107932.

Flourakis M, Allada R. Patch-clamp electrophysiology in Drosophila circadian pacemaker neurons. Methods Enzymol, 2015; 552: 23–44. [PubMed: 25707271]

Flourakis M, Kula-Eversole E, Hutchison AL, Han TH, Aranda K, Moose DL, White KP, Dinner AR, Lear BC, Ren D, Diekman CO, Raman IM, Allada R. A Conserved Bicycle Model for Circadian Clock Control of Membrane Excitability. Cell, 2015; 162: 836–48. [PubMed: 26276633]

Fogle KJ, Parson KG, Dahm NA, Holmes TC. CRYPTOCHROME is a blue-light sensor that regulates neuronal firing rate. Science, 2011; 331: 1409–13. [PubMed: 21385718]

Gouwens NW, Wilson RI. Signal propagation in Drosophila central neurons. J Neurosci, 2009; 29: 6239–49. [PubMed: 19439602]

Granger CWJ. Some Properties of Time-Series Data and Their Use in Econometric-Model Specification. J Econometrics, 1981; 16: 121–30.

Guo F, Holla M, Diaz MM, Rosbash M. A Circadian Output Circuit Controls Sleep-Wake Arousal in Drosophila. Neuron, 2018; 100: 624–35 e4. [PubMed: 30269992]

Guo F, Yu J, Jung HJ, Abruzzi KC, Luo W, Griffith LC, Rosbash M. Circadian neuron feedback controls the Drosophila sleep--activity profile. Nature, 2016; 536: 292–7. [PubMed: 27479324]

Hamada S, Tabuchi M, Toyota T, Sakurai T, Hosoi T, Nomoto T, Nakatani K, Fujinami M, Kanzaki R. Giant vesicles functionally expressing membrane receptors for an insect pheromone. Chem Commun (Camb), 2014; 50: 2958–61. [PubMed: 24509495]

Hamill OP, Marty A, Neher E, Sakmann B, Sigworth FJ. Improved patch-clamp techniques for high-resolution current recording from cells and cell-free membrane patches. Pflugers Arch, 1981; 391: 85–100. [PubMed: 6270629]

Hasebe M, Yoshino M. Nitric oxide/cGMP/PKG signaling pathway activated by M1-type muscarinic acetylcholine receptor cascade inhibits Na+-activated K+ currents in Kenyon cells. J Neurophysiol, 2016; 115: 3174–85. [PubMed: 26984419]

Hess S, Pouzat C, Kloppenburg P. Datasets for calcium dynamics comparison between the whole-cell and a beta-escin based perforated patch configuration in brain slices from adult mice. Data Brief, 2021; 39: 107494. [PubMed: 34754890]

Ho MCW, Tabuchi M, Xie X, Brown MP, Luu S, Wang S, Kolodkin AL, Liu S, Wu MN. Sleep need-dependent changes in functional connectivity facilitate transmission of homeostatic sleep drive. Curr Biol, 2022; 32: 4957–66 e5. [PubMed: 36240772]

Hodgkin AL, Huxley AF. A quantitative description of membrane current and its application to conduction and excitation in nerve. J Physiol, 1952; 117: 500–44. [PubMed: 12991237]

Horn R, Marty A. Muscarinic activation of ionic currents measured by a new whole-cell recording method. J Gen Physiol, 1988; 92: 145–59. [PubMed: 2459299]

Inoue S, Murata K, Tanaka A, Kakuta E, Tanemura S, Hatakeyama S, Nakamura A, Yamamoto C, Hasebe M, Kosakai K, Yoshino M. Ionic channel mechanisms mediating the intrinsic excitability of Kenyon cells in the mushroom body of the cricket brain. J Insect Physiol, 2014; 68: 44–57. [PubMed: 24995840]

Jayant K, Hirtz JJ, Plante IJ, Tsai DM, De Boer WD, Semonche A, Peterka DS, Owen JS, Sahin O, Shepard KL, Yuste R. Targeted intracellular voltage recordings from dendritic spines using quantum-dot-coated nanopipettes. Nat Nanotechnol, 2017; 12: 335–42. [PubMed: 27941898]

Jayant K, Wenzel M, Bando Y, Hamm JP, Mandriota N, Rabinowitz JH, Plante IJ, Owen JS, Sahin O, Shepard KL, Yuste R. Flexible Nanopipettes for Minimally Invasive Intracellular Electrophysiology In Vivo. Cell Rep, 2019; 26: 266–78 e5. [PubMed: 30605681]

Lamaze A, Kratschmer P, Chen KF, Lowe S, Jepson JEC. A Wake-Promoting Circadian Output Circuit in Drosophila. Curr Biol, 2018; 28: 3098–105 e3. [PubMed: 30270186]

Lamaze A, Stanewsky R. DN1p or the "Fluffy" Cerberus of Clock Outputs. Front Physiol, 2019; 10: 1540. [PubMed: 31969832]

Lei CL, Clerx M, Whittaker DG, Gavaghan DJ, de Boer TP, Mirams GR. Accounting for variability in ion current recordings using a mathematical model of artefacts in voltage-clamp experiments. Philos Trans A Math Phys Eng Sci, 2020; 378: 20190348. [PubMed: 32448060]

Li C A reliable whole cell clamp technique. Adv Physiol Educ, 2008; 32: 209–11. [PubMed: 18794242]

Li WC, Soffe SR, Roberts A. A direct comparison of whole cell patch and sharp electrodes by simultaneous recording from single spinal neurons in frog tadpoles. J Neurophysiol, 2004; 92: 380–6. [PubMed: 14999043]

Lindau M, Fernandez JM. IgE-mediated degranulation of mast cells does not require opening of ion channels. Nature, 1986; 319: 150–3. [PubMed: 2417125]

McCarthy EV, Wu Y, Decarvalho T, Brandt C, Cao G, Nitabach MN. Synchronized bilateral synaptic inputs to Drosophila melanogaster neuropeptidergic rest/arousal neurons. J Neurosci, 2011; 31: 8181–93. [PubMed: 21632940]

Murthy M, Turner G. Dissection of the head cuticle and sheath of living flies for whole-cell patch-clamp recordings in the brain. Cold Spring Harb Protoc, 2013a; 2013: 134–9. [PubMed: 23378645]

Murthy M, Turner G. Whole-cell in vivo patch-clamp recordings in the Drosophila brain. Cold Spring Harb Protoc, 2013b; 2013: 140–8. [PubMed: 23378646]

Nakamura A, Yoshino M. A novel GABAergic action mediated by functional coupling between GABAB-like receptor and two different high-conductance K+ channels in cricket Kenyon cells. J Neurophysiol, 2013; 109: 1735–45. [PubMed: 23303861]

Neher E, Sakmann B. Single-channel currents recorded from membrane of denervated frog muscle fibres. Nature, 1976; 260: 799–802. [PubMed: 1083489]

Nguyen DL, Hutson AN, Zhang Y, Daniels SD, Peard AR, Tabuchi M. Age-Related Unstructured Spike Patterns and Molecular Localization in Drosophila Circadian Neurons. Front Physiol, 2022; 13: 845236. [PubMed: 35356078]

Noireaux V, Libchaber A. A vesicle bioreactor as a step toward an artificial cell assembly. Proc Natl Acad Sci U S A, 2004; 101: 17669–74. [PubMed: 15591347]

Priel A, Gil Z, Moy VT, Magleby KL, Silberberg SD. Ionic requirements for membrane-glass adhesion and giga seal formation in patch-clamp recording. Biophys J, 2007; 92: 3893–900. [PubMed: 17369408]

Proakis J, Manolakis D. Digital Signal Processing: Principles, Algorithms, and Applications. Prentice-Hall, Inc.: United States, 2006.

Robinson JT, Jorgolli M, Shalek AK, Yoon MH, Gertner RS, Park H. Vertical nanowire electrode arrays as a scalable platform for intracellular interfacing to neuronal circuits. Nat Nanotechnol, 2012; 7: 180–4. [PubMed: 22231664]

Roemmich AJ, Schutte SS, O'Dowd DK. Ex vivo Whole-cell Recordings in Adult Drosophila Brain. Bio Protoc, 2018; 8.

Ryglewski S, Duch C. Preparation of Drosophila central neurons for in situ patch clamping. J Vis Exp, 2012.

Sakmann B, Neher E. Patch clamp techniques for studying ionic channels in excitable membranes. Annu Rev Physiol, 1984; 46: 455–72. [PubMed: 6143532]

Sarantopoulos C, McCallum JB, Kwok WM, Hogan Q. Beta-escin diminishes voltage-gated calcium current rundown in perforated patch-clamp recordings from rat primary afferent neurons. J Neurosci Methods, 2004; 139: 61–8. [PubMed: 15351522]

Seluzicki A, Flourakis M, Kula-Eversole E, Zhang L, Kilman V, Allada R. Dual PDF signaling pathways reset clocks via TIMELESS and acutely excite target neurons to control circadian behavior. PLoS Biol, 2014; 12: e1001810. [PubMed: 24643294]

Shafer OT, Keene AC. The Regulation of Drosophila Sleep. Curr Biol, 2021; 31: R38–R49. [PubMed: 33434488]

Shahidullah M, Reddy S, Fei H, Levitan IB. In vivo role of a potassium channel-binding protein in regulating neuronal excitability and behavior. J Neurosci, 2009; 29: 13328–37. [PubMed: 19846720]

Sheeba V, Gu H, Sharma VK, O'Dowd DK, Holmes TC. Circadian- and light-dependent regulation of resting membrane potential and spontaneous action potential firing of Drosophila circadian pacemaker neurons. J Neurophysiol, 2008; 99: 976–88. [PubMed: 18077664]

Sigworth FJ. The patch clamp is more useful than anyone had expected. Fed Proc, 1986; 45: 2673–7. [PubMed: 2429870]

Sigworth FJ, Neher E. Single Na+ channel currents observed in cultured rat muscle cells. Nature, 1980; 287: 447–9. [PubMed: 6253802]

Sokabe M, Sachs F, Jing ZQ. Quantitative video microscopy of patch clamped membranes stress, strain, capacitance, and stretch channel activation. Biophys J, 1991; 59: 722–8. [PubMed: 1710939]

Staley KJ, Otis TS, Mody I. Membrane properties of dentate gyrus granule cells: comparison of sharp microelectrode and whole-cell recordings. J Neurophysiol, 1992; 67: 1346–58. [PubMed: 1597717]

Suchyna TM, Markin VS, Sachs F. Biophysics and structure of the patch and the gigaseal. Biophys J, 2009; 97: 738–47. [PubMed: 19651032]

Svoboda K, Helmchen F, Denk W, Tank DW. Spread of dendritic excitation in layer 2/3 pyramidal neurons in rat barrel cortex in vivo. Nat Neurosci, 1999; 2: 65–73. [PubMed: 10195182]

Tabuchi M Dynamic neuronal instability generates synaptic plasticity and behavior: Insights from Drosophila sleep. Neurosci Res, 2023.

Tabuchi M, Coates KE, Bautista OB, Zukowski LH. Light/Clock Influences Membrane Potential Dynamics to Regulate Sleep States. Front Neurol, 2021; 12: 625369. [PubMed: 33854471]

Tabuchi M, Monaco JD, Duan G, Bell B, Liu S, Liu Q, Zhang K, Wu MN. Clock-Generated Temporal Codes Determine Synaptic Plasticity to Control Sleep. Cell, 2018; 175: 1213–27 e18. [PubMed: 30318147]

Thieffry M, Neyton J, Pelleschi M, Fevre F, Henry JP. Properties of the mitochondrial peptide-sensitive cationic channel studied in planar bilayers and patches of giant liposomes. Biophys J, 1992; 63: 333–9. [PubMed: 1384736]

Thomas MV. Microelectrode amplifier with improved method of input-capacitance neutralisation. Med Biol Eng Comput, 1977; 15: 450–4. [PubMed: 197341]

Wilson RI, Turner GC, Laurent G. Transformation of olfactory representations in the Drosophila antennal lobe. Science, 2004; 303: 366–70. [PubMed: 14684826]

Highlights

- Glass electrodes with a phospholipid membrane coating are inspired.

- Membrane-coated electrodes are based on a newly developed tip-dip protocol.

- Membrane-coated glass electrodes make intracellular electrophysiology more stable.

- Single-channel recordings show an improved signal-to-noise ratio in the recordings of membrane-coated electrodes.
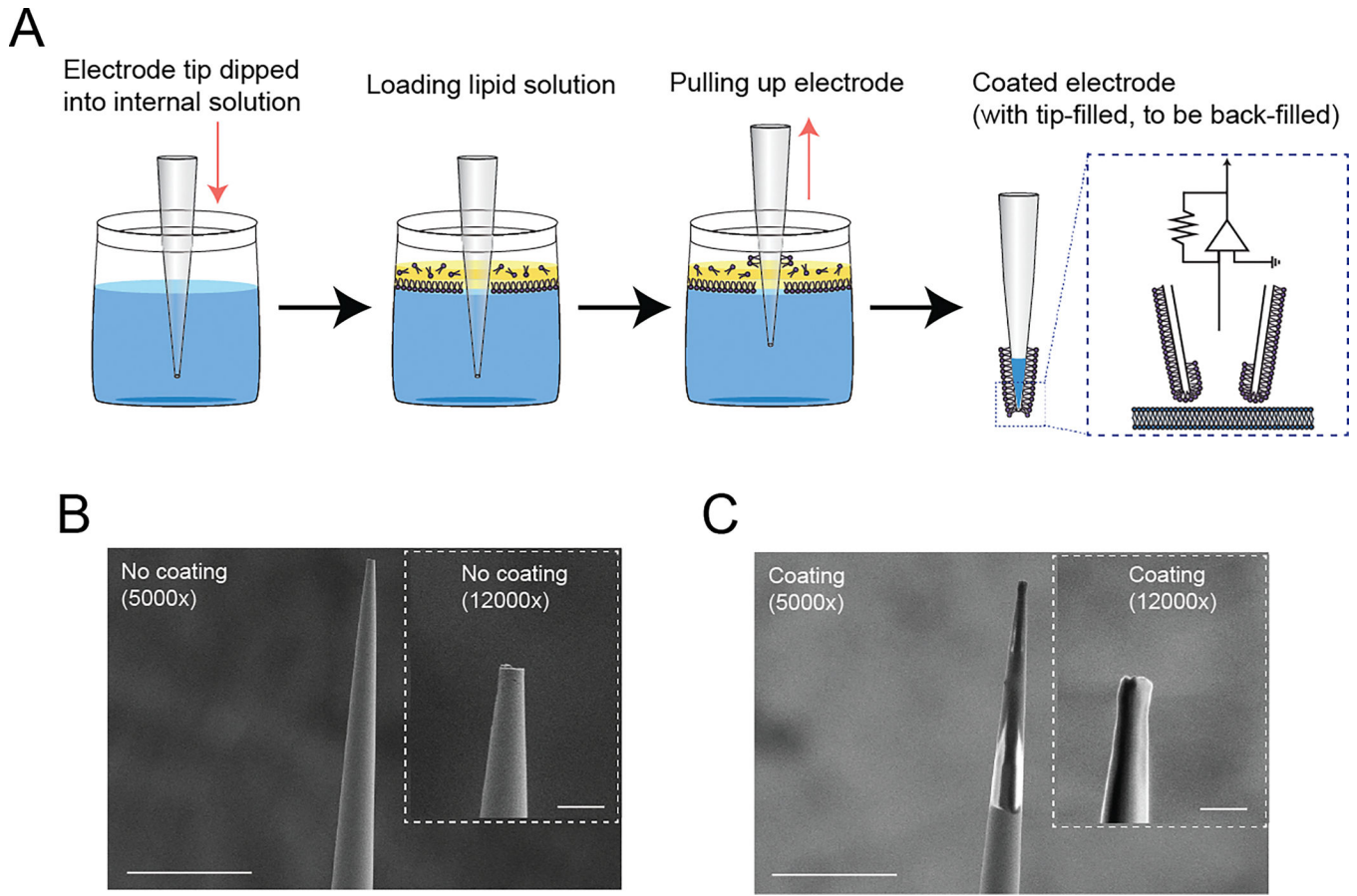
Figure 1.
Development of a membrane-coated glass electrode. (**A**) Graphical schematics of the coating process of the membrane-coated electrodes. The process is initiated by immersing the electrode tip into a reservoir containing a standard internal electrode solution. At the interface between the water and oil phases, a single phospholipid monolayer is expected to form (Noireaux and Libchaber, 2004). After adding a minimized layer of the prepared lipid solution onto the surface of the internal electrode solution, the electrode is vertically lifted using the micromanipulator. The resulting membrane-coated electrodes were promptly employed for electrophysiological recording, after the standard backfilling procedure with the internal electrode solution. (**B**) Surface visualization of an uncoated glass electrode at 5,000x magnification and 12,000x magnification (inset). Scale bar indicates 20 μm at 5,000x magnification and 2.5 μm at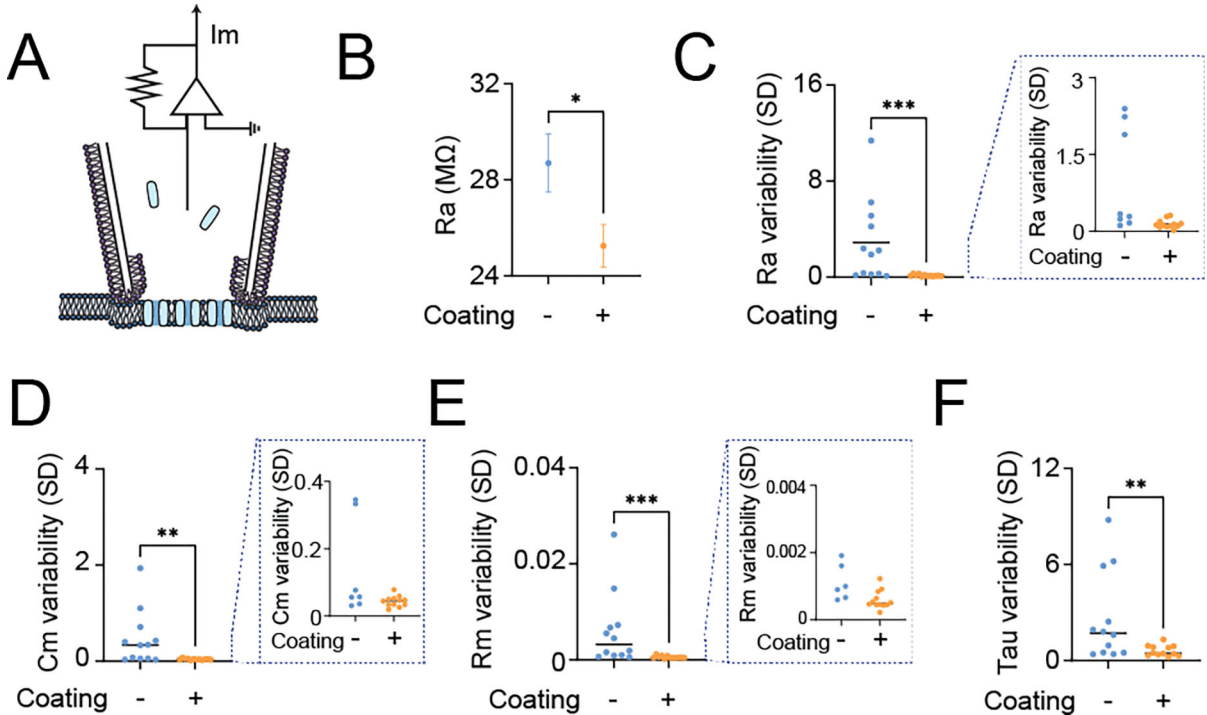 12,000x magnification (inset). (**C**) Surface visualization of a membrane-coated glass electrode at 5,000x magnification and 12,000x magnification (inset). Scale bar indicates 20 μm at 5,000x magnification and 2.5 μm at 12,000x magnification (inset).

Figure 2.

Quantification of the variability of passive membrane properties to evaluate the membrane-coated electrode performance under voltage-clamp mode of perforated patch clamp recordings. (**A**) Graphical diagrams of the recording configuration. The blue represents Escin, the perforating agent that creates chemical pores on the neuronal membrane underneath the electrode. (**B**) Comparison of the mean value of access resistance (Ra) during the membrane test with (+) or without (−) membrane coating, (**C**) Comparison of the standard deviation of Ra during the membrane test with (+) or without (−) membrane coating, (**D**) Comparison of the standard deviation of membrane capacitance (Cm) during the membrane test with (+) or without (−) membrane coating, (**E**) Comparison of the standard deviation of membrane resistance (Rm) during the membrane test with (+) or without (−) membrane coating, and (**F**) Comparison of the standard deviation of membrane time constant (Tau) during the membrane test with (+) or without (−) membrane coating. All data are obtained from the membrane test using the voltage-clamp mode of perforated patch clamp recordings from DN1p circadian clock neurons in Drosophila, by using standard patch-electrodes with (+) membrane-coated electrodes (N=12) and without (−) membrane coating (N=12). One DN1 neuron was recorded per fly. Single-electrode recordings were performed in random order between no coating and coating. Each inset (dashed line) shows a zoomed subplot. The statistics are Mann–Whitney U test with *p < 0.05, **p < 0.01, and ***p < 0.001.
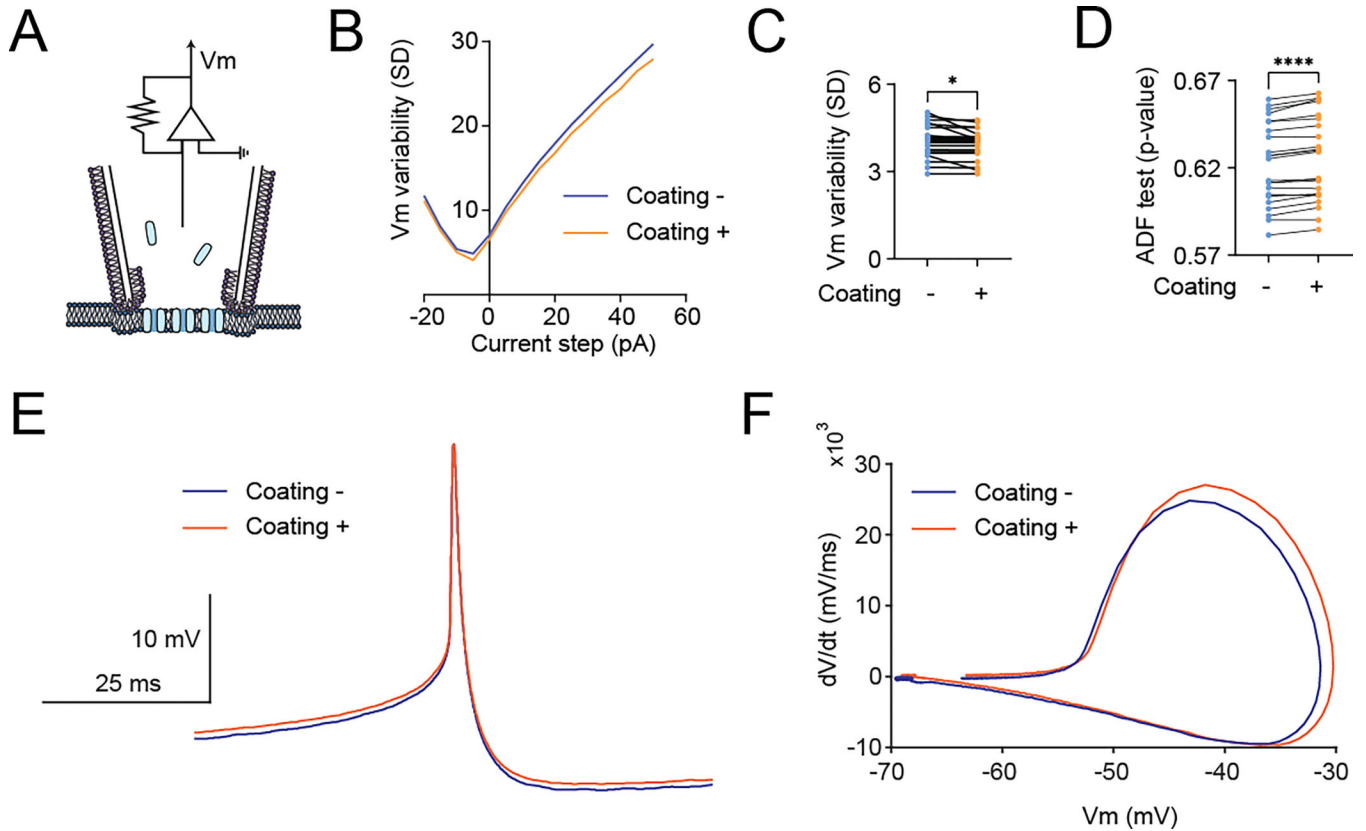
Figure 3.

Quantification of the variability of membrane potential (Vm) dynamics to evaluate the membrane-coated electrode performance under the current-clamp mode of perforated patch clamp recordings. (**A**) Graphical diagrams of the recording configuration. The blue represents Escin, the perforating agent that creates chemical pores on the neuronal membrane underneath the electrode. (**B**) Comparison of the mean value of Vm variability in response to stepping current injections with (+) or without (−) membrane coating, (**C**) Comparison of Vm variability in the resting states with zero current injection ("I zero" mode), and (**D**) Comparison of time-serious data of Vm p-values of an augmented Dickey–Fuller test (ADF) tests under the current-clamp mode of perforated patch clamp recordings with (+) or without (−) membrane coating. (**E**) Averaged Vm traces sorted based on action potential timing obtained from the current-clamp mode of perforated patch clamp recordings with (orange) or without (blue) membrane coating glass electrodes. (**F**) Averaged phase plots (dV/dt versus Vm) of action potential from the current-clamp mode of perforated patch clamp recordings with (orange) or without (blue) membrane coating glass electrodes. All data are obtained from the current-clamp mode of perforated patch clamp recordings from DN1p circadian clock neurons in Drosophila, by using standard patch-electrodes with (+) membrane-coated electrodes (N=24) and without (−) membrane coating (N=24). One DN1 neuron was simultaneously recorded from two electrodes per fly. Simultaneous recordings were performed by using membrane-coated and control electrodes. The statistics are paired t-test with *$p < 0.05$ and ****$p < 0.001$.
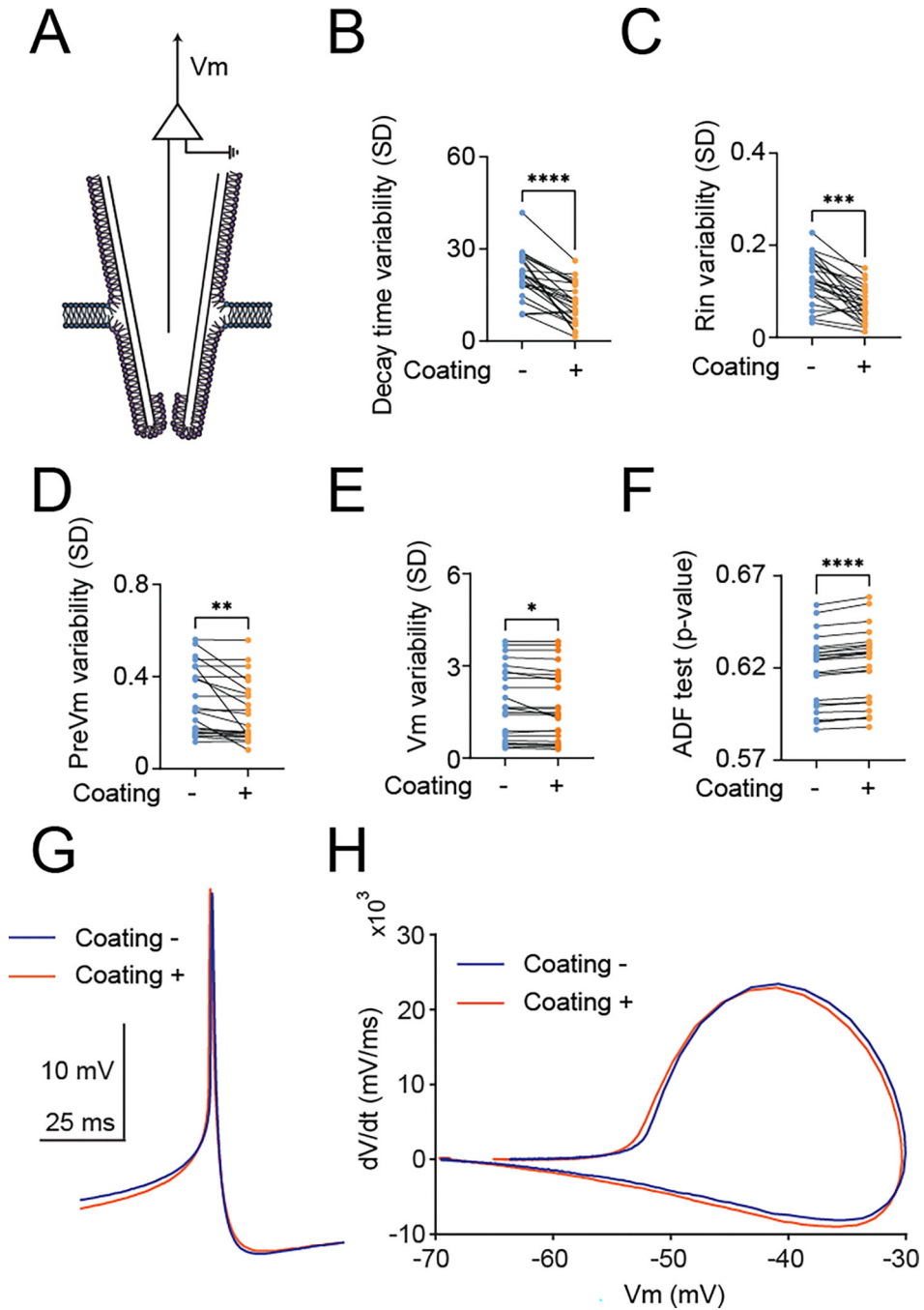
Figure 4.
Quantification of the variability of membrane potential (Vm) dynamics to evaluate the membrane-coated electrode performance under the current-clamp mode of sharp electrode recordings. (**A**) Graphical diagrams of the recording configuration. (**B**) Comparison of the variability of the decay time constant of Vm in response to depolarizing current injections with (+) or without (−) membrane coating, (**C**) Comparison of the variability of the input resistance in response to hyperpolarizing current injections with (+) or without (−) membrane coating, (**D**) Comparison of Vm variability during hyperpolarizing prepulse

injection ("PreVm") with (+) or without (−) membrane coating, (**E**) Comparison of Vm variability in the resting states with zero current injection ("I zero" mode), and (**F**) Comparison of time-series data of Vm p-values of an ADF tests under the current-clamp mode of the sharp electrode with (+) or without (−) membrane coating. (**G**) Averaged Vm traces sorted based on action potential timing obtained from the current-clamp mode of sharp electrode recordings with (orange) or without (blue) membrane coating glass electrodes. (**H**) Averaged phase plots (dV/dt versus Vm) of action potential from the current-clamp mode of sharp electrode recordings with (orange) or without (blue) membrane coating glass electrodes. All data are obtained from the current-clamp mode of sharp electrode recordings from DN1p circadian clock neurons in Drosophila, by using standard sharp electrodes with (+) membrane-coated electrodes (N=24) and without (−) membrane coating (N=24). One DN1 neuron was simultaneously recorded from two electrodes per fly. Simultaneous recordings were performed by using membrane-coated and control electrodes. The statistics are paired t-test with $*p < 0.05$, $**p < 0.01$, $***p < 0.001$, and $****p < 0.0001$.
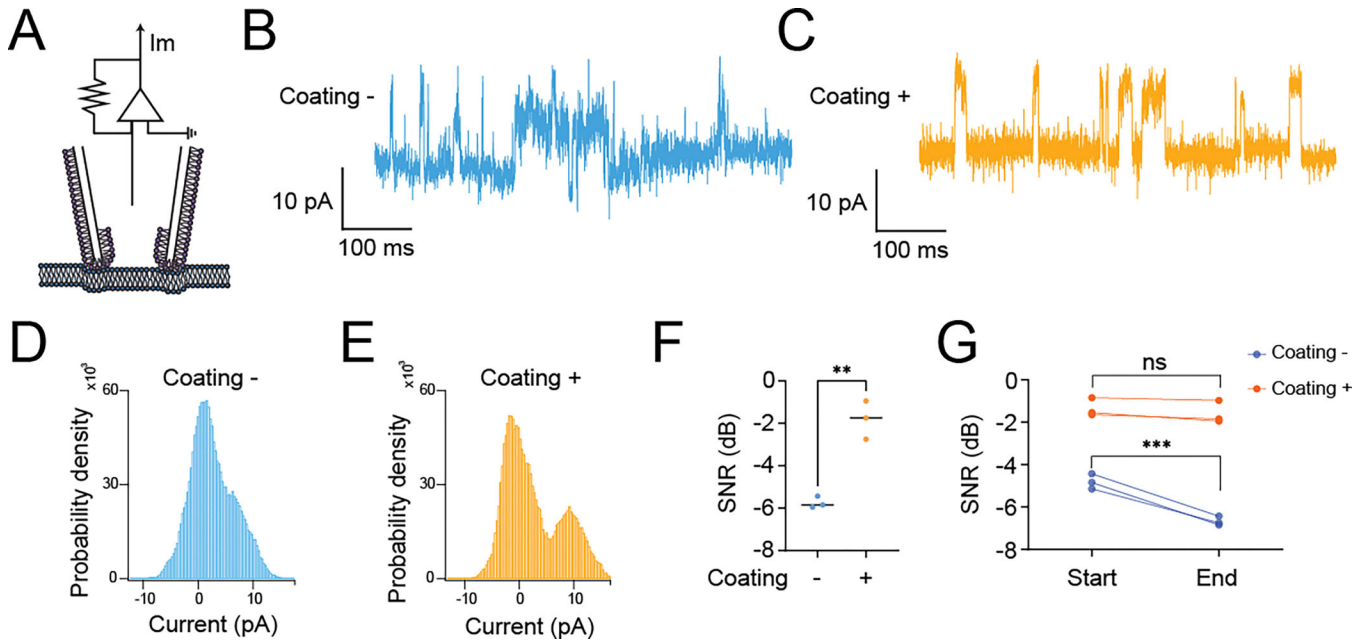
Figure 5.
Quantification of the variability of single-channel membrane current (Im) dynamics to evaluate the membrane-coated electrode performance under the voltage-clamp mode of cell-attached recordings. (**A**) Graphical diagrams of the recording configuration. (**B**) Representative current trace of Im obtained by using standard patch electrode (**C**) Representative current trace of Im obtained by using membrane-coated electrode (**D**) All-points histogram of Im obtained by using standard patch electrode (**E**) All-points histogram of Im obtained by using membrane-coated electrode (**F**) Comparison of the signal-to-noise ratio (SNR) in Im with (+) or without (−) membrane coating. The SNR was assessed in decibels relative to the carrier wave (dBc). This measurement was derived from a real-valued sinusoidal Im determined by a modified periodogram using a Kaiser window with a β value of 38, corresponding to the length of the input signal. (**G**) Comparison between the start and end points of (SNR) in Im with (+) or without (−) membrane coating. During the entire recording period of 1 minute, we took the first 10 seconds as the start point and the last 10 seconds as the endpoint. All data are obtained from the voltage-clamp mode of cell-attached recordings from DN1p circadian clock neurons in Drosophila, by using standard patch electrodes with (+) membrane-coated electrodes (N=3) and without (−) membrane coating (N=3). Single-channel membrane current was evoked by a single-step pulse change from −70 mV holding potential to +60 mV holding potential. One DN1 neuron was recorded per fly. Single-electrode recordings were performed in random order between no coating and coating. The statistics are unpaired t-test with **p < 0.01 (F) and two-way ANOVA with Šídák's multiple comparisons test with ***p < 0.001 and ns indicates non-significance (G).